Hindawi
Journal of Nanomaterials
Volume 2021, Article ID 6655375, 11 pages
https://doi.org/10.1155/2021/6655375

Research Article

Investigating the Anti-Inflammatory Activity of Curcumin-Loaded Silica-Containing Redox Nanoparticles

Khoa Minh Le,[1,2] Nhu-Thuy Trinh,[1,2] Vinh Dinh-Xuan Nguyen,[1,2] Tien-Dat Van Nguyen,[1,2] Thu-Ha Thi Nguyen,[1,2] Toi Van Vo,[1,2] Tuan Quoc Tran,[2,3] Dai-Nghiep Ngo,[2,3] and Long Binh Vong[1,2]

[1]*School of Biomedical Engineering, International University, 700000 Ho Chi Minh, Vietnam*
[2]*Vietnam National University Ho Chi Minh City (VNU-HCMC), 700000 Ho Chi Minh, Vietnam*
[3]*Faculty of Biology and Biotechnology, University of Science, 700000 Ho Chi Minh, Vietnam*

Correspondence should be addressed to Long Binh Vong; vblong@hcmiu.edu.vn

Received 6 December 2020; Revised 6 January 2021; Accepted 19 January 2021; Published 31 January 2021

Academic Editor: Duong Tuan Quang

Chronic inflammation is considered as one of the challenging diseases, and overproduction of reactive oxygen species (ROS) is strongly related to the onset of chronic inflammation. Therefore, antioxidant and anti-inflammatory approaches are particularly becoming suitable treatment and prevention of inflammation. Curcumin (CUR), a main component of turmeric extract, is well known as an effective agent in both antioxidant and anti-inflammatory activities; however, there are still some limitations of its use including poor water solubility, low bioavailability, and oxidation by ROS. Nanotechnology has been used as a drug delivery system, which is a promising approach in overcoming the aforementioned drawbacks of CUR; hence, it improves the antioxidant and anti-inflammatory effects of conventional medications. In this research, silica-containing redox nanoparticles (siRNP) were designed with the size of several tens of nanometers, prepared by self-assembly of an amphiphilic block copolymer consisting of drug absorptive silica moiety and ROS-scavenging nitroxide radical moiety in the hydrophobic segment. CUR was simply encapsulated into siRNP through the dialysis method, creating CUR-loaded siRNP (CUR@siRNP), which significantly improved the water solubility of CUR. The efficient antioxidant activity and anti-inflammatory effect of CUR@siRNP *in vitro* were also improved via 2,2-diphenyl-1-picrylhydrazyl assay and lipopolysaccharide-induced macrophage cell line activation, respectively. Oral administration of CUR@siRNP showed improvement in pharmacokinetic profile *in vivo* including AUC and C_{max} values as compared to free CUR. Furthermore, the anti-inflammatory effect of nanoformulation was investigated in the colitis mouse model induced by dextran sodium sulfate.

1. Introduction

According to the World Health Organization (WHO), chronic inflammation is considered one of the greatest threats to other chronic diseases. Inflammation acts as a vital part of the immune system's response to injury and infection, by which the immune system detects and eliminates harmful stimuli while initiating wound healing [1]. Prolonged inflammation, or chronic inflammation, is characterized for long-term persistence from months, years to even decades. Moreover, chronic inflammation is strongly related to many challenging diseases, such as cancer, heart disease, diabetes, and Alzheimer's disease [2]. The discovery of reactive oxygen species (ROS) features its active roles in many pathways, including oxidative stress, which progressed chronic inflammation. It has been reported that oxidative stress or overproduced ROS accumulatively induces chronic inflammation as both signalling molecules and inflammatory mediators [3]. ROS are defined as highly reactive oxygen radicals, such as superoxide (O_2^-) or hydroxyl radical ($OH^\bullet$), which display various reactivity. Due to a single electron on the outer shell, ROS are unstable and may react with adjacent molecules to maintain electrical homeostasis [4]. Endogenous ROS accumulation activates thioredoxin, which interacted protein (TXNIP) complex [4]. The complex detached, enabling TXNIP to bind with NLRP3 inflammasome. Furthermore,

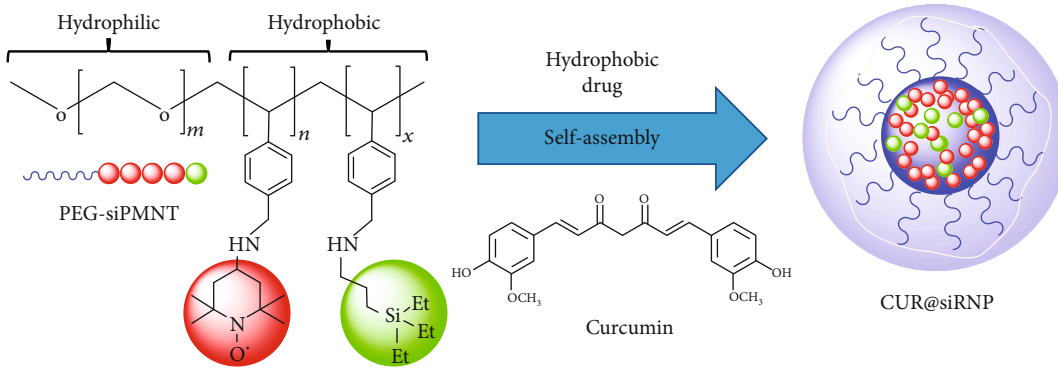

Figure 1: The self-assembly of curcumin-loaded silica-containing redox nanoparticle (CUR@siRNP).

the combination of NLRP3, apoptosis-associated speck-like protein, and caspase-1 proteins activated NLRP3 to induce production of IL-1β and IL-18, both are secreted by inflammatory cells, then promoting inflammation. ROS oxidizes crucial signalling protein in inflammation sites, i.e., tyrosine phosphatase, which results in endothelial dysfunction and tissue injury. Also, oxidative stress disrupts interendothelial junction, while inducing inflammatory cell migration across endothelial barriers to assist pathogen clearance. Hence, these consequences cause damage to biomolecules and severe tissue injury, resulting in inflammatory diseases.

Curcumin (CUR), a polyphenolic component of turmeric extract, has been mainly used as a commercial dietary additive and supplement. In addition, CUR enhances physiological antioxidant mechanism, while preventing essential inflammatory molecules, therefore, downregulating inflammation altogether [5]. Despite all of the advantages, its clinical application has been impeded by many drawbacks. CUR is great insoluble in water, poor absorption, rapid metabolism, short biological half-life, and spontaneous oxidative degradation caused by ROS leading to its low bioavailability [6, 7]. In order to improve CUR solubility, many approaches have been considered. One attempt by adding adjuvants, a combination of CUR and other bioenhancers, such as piperine, quercetin, or silibinin was used to enhance cellular absorption. This increment of pharmacokinetics is made possible by albumin-binding interactions [8]. Unfortunately, some bioenhancers showed toxicity in experimental animals. Alternately, the search for developed drug delivery nanotechnologies is perceived as a highlight approach. Nanoparticles have shown promising drug solubility enhancement properties and cell-specific distribution, hence, improving therapeutic effect [9]. There have been versatile forms and nanoparticle structures, including liposomes, dendrimers, and solid lipid nanoparticles developed for biomedical applications. The greatest challenge in nanoparticle-based pharmaceutical engineering is designing a stable and controlled release drug delivery system [10]. Conventional drug delivery systems faced coherent drawbacks, such as low drug loading capacity, low durability, and adverse side-effects. These have been used as a nanocarrier for CUR to overcome its aforementioned drawbacks. The first attempt was from Kanai et al. (2011), who used a nanoparticle formulation called THERACURMIN to illustrate the improvement in bioavailability in human subjects [11]. Tai et al. (2019) recently formulated curcumin-loaded liposomal nanoparticles (Cur-LP) with the same objective. In order to improve drug bioavailability, the research coated liposome nanoparticles with high molecular weight chitosan to enhance stability and maintain the release capacity of Cur-LP [12]. Nevertheless, various designed nanoparticles shared common concerns: they exhibited low stability, whereas the release profile was inconsistent and uncontrollable. In addition, their loading capacity was barely insufficient due to the instability, which leads to poor therapeutic effect. Finally, nanoparticle cytotoxicity still remained as a great struggle, with complex nanocarrier may engage unwanted immune responses, therefore, it adversely effects on overall health [13]. A designed silica-containing redox nanoparticle (siRNP) was previously developed to enhance therapeutic drugs with low bioavailability. siRNP was formed from self-assembled amphiphilic polymer (PEG-siPMNT, polyethylene glycol-*b*-poly (4-[2,2,6,6-tetramethyl piperidine-1-oxyl] aminomethyl styrene) composed of hydrophilic PEG segment and hydrophobic segment consisting of a ROS-scavenging moiety and a silica moiety for stability encapsulation (Figure 1) [14, 15]. This represents a self-assembly micelle structure, where the hydrophobic drug is captured within the core of the nanocarrier [15]. The objective of this study was to investigate the bioavailability and anti-inflammatory effects of CUR-loaded siRNP (CUR@siRNP) compared to free CUR. The results showed that CUR@siRNP significantly improved the water solubility and bioavailability of CUR after oral administration. Consequently, CUR@siRNP exhibited a promising antioxidant and anti-inflammatory effects *in vitro* of RAW 264.7 cell activation and *in vivo* of dextran sodium sulfate- (DSS-) induced colitis model in mice.

2. Materials and Methods

2.1. Synthesis of Nanoparticles. The synthesis of silica-containing redox polymer (PEG-siPMNT) was described in the previous study [14]. siRNP and CUR@siRNP were synthesized through dialysis of PEG-siPMNT polymer against distilled water. Briefly, 0.5 mL PEG-siPMNT (60 mg/mL) was well-mixed with 0.5 mL dimethylformamide (DMF, FUJIFILM Wako Chemicals—Japan) to prepare siRNP. The solution was transferred into the dialysis membrane and

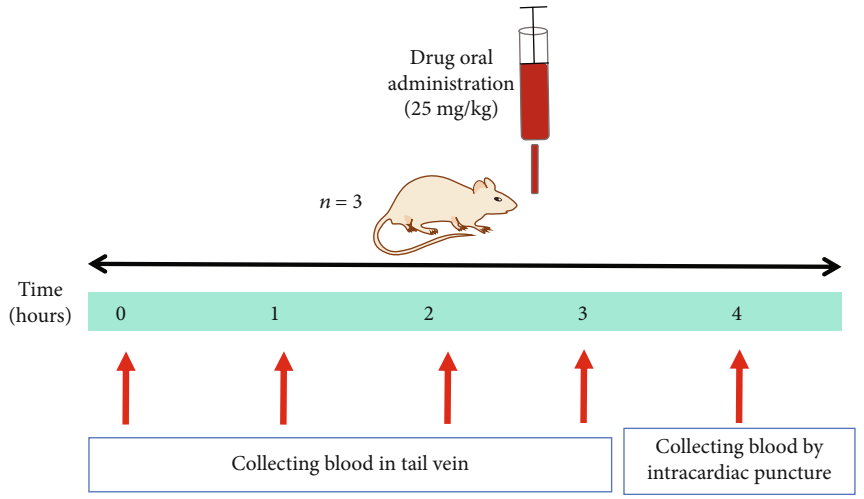

Figure 2: Timeline for blood sample collection of the CUR-treated group and the CUR@siRNP-treated group (25 mg/kg) for the pharmacokinetic experiment.

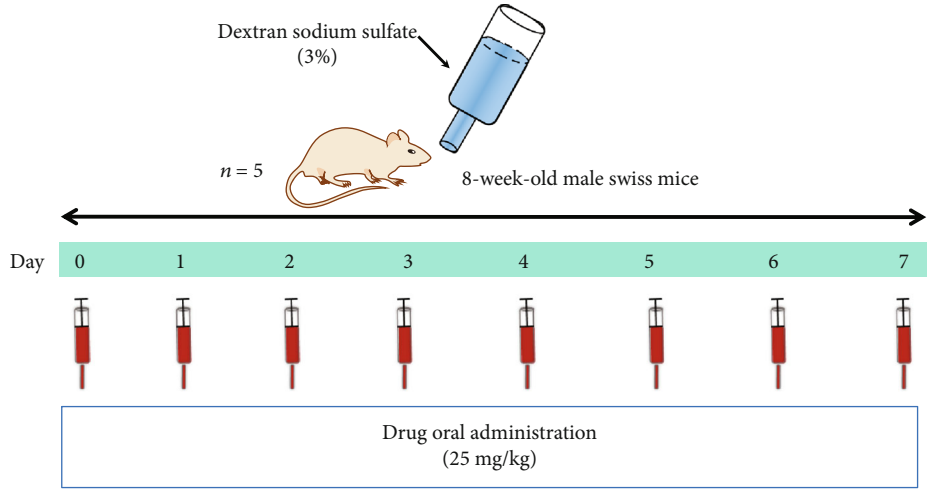

Figure 3: The oral administration of CUR and CUR@siRNP (25 mg/kg) in a colitis mouse model induced by dextran sodium sulfate (DSS).

Table 1: Disease activity index (DAI) scores [18, 19].

Stool consistency	Feces bleeding	Weight loss
		0 = no weight loss
0 = formed	0 = normal colour	1 = 1% – 5% weight loss
1 = mild soft	1 = brown colour stool	2 = 6% – 10% weight loss
2 = very soft	2 = reddish colour stool	3 = 11% – 15% weight loss
3 = watery	3 = bloody stool	4 = ≥16% weight loss

proceeded the dialysis for 24 h with occasional water change. CUR@siRNP was prepared by a similar method, whereas CUR (Tokyo Chemical Industry, Japan) was encapsulated via the hydrophobic interaction and the drug absorption feature of silica core of siRNP [15]. In such, 1.5 mg of CUR was fully dissolved in 0.5 mL of DMF. Next, 0.5 mL of PEG-siPMNT (60 mg/mL) and 14 μL of tetraethyl orthosilicate (TEOS—St. Louis, MO, USA) were added to the mixture. Obtained substance was dialyzed against water for 24 h with an occasional water change.

2.2. Characteristics of CUR@siRNP

2.2.1. Particle Size. The particle size of CUR@siRNP was analyzed by dynamic light scattering (DLS) using Zetasizer ZS (Malvern, UK). The CUR@siRNP samples were diluted in water or PBS, and the measurement was performed with an angle of 173° at 25°C.

2.2.2. Measurement of Encapsulation Efficiency and Loading Capacity. CUR concentration presented in the siRNP was measured at 450 nm and expressed in terms of encapsulation efficiency (EE) and loading capacity (LC). CUR standard curve was constructed with serial dilution of CUR in DMSO solution (0, 10, 20, 40, 50, and 60 μg/mL). CUR@siRNP was diluted with distilled water, and all samples were measured at 450 nm using UV-VIS spectrophotometer (Thermo Fisher

Table 2: Histological scores [20, 21].

Crypt architecture	Cellular infiltration	Goblet cell depletion
0 = normal	0 = normal	
1 = minimal crypt distortion	1 = minimal cellular infiltration	0 = absent
2 = moderate crypt distortion	2 = moderate cellular infiltration	1 = present
3 = severe crypt distortion	3 = dense cellular infiltration	

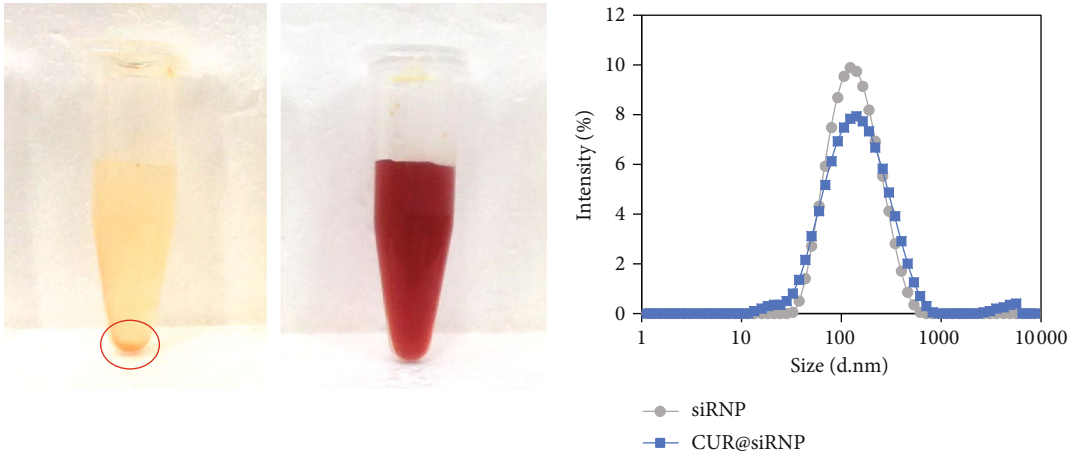

Figure 4: Characterization of CUR@siRNP. (a) The solubility of CUR (left) and CUR@siRNP (right) in water (at 1 mg/mL concentration of CUR). The red circle indicates the insoluble curcumin particles. (b) The size distribution of siRNP and CUR@siRNP was measured by DLS.

Table 3: Summary of the size of siRNP and CUR@siRNP, including encapsulation efficiency (EE) and loading capacity (LC) of CUR@siRNP.

Sample	Size (nm)	PdI	EE (%)	LC (%)
siRNP	122±1	0.26	—	—
CUR@siRNP	142 ± 1	0.30	74.3 ± 5.1	7.4 ± 0.5

Scientific). The EE and LC were calculated using the given formulas:

$$\text{EE}\,(\%) = \frac{\text{The mass of drug encapsulated}}{\text{Initial drug mass}} \text{ x } 100\%,$$
$$\text{LC}\,(\%) = \frac{\text{The mass of drug encapsulated}}{\text{Initial polymer mass}} \text{ x } 100\%. \quad (1)$$

2.3. Investigation of CUR@siRNP Bioactivities

2.3.1. Antioxidant Assay. Antioxidant activity of CUR@siRNP was determined using the radical scavenging ability towards 2,2-diphenyl-1-picrylhydrazyl (DPPH—Sigma Aldrich, St. Louis, MO, USA). In this study, 50 μL of CUR in DMSO, siRNP, and CUR@siRNP in various concentrations (0, 2, 5, 8, and 10 μg/mL) were well-mixed with 150 μL of DPPH solution (40 μg/mL). Other samples treated with vitamin C served as the positive control, while distilled water acted as the negative control. All samples were incubated for 30 minutes in dark condition at room temperature. The optical density (OD) of tested samples was measured at 517 nm afterward, and the percentage of DPPH scavenging capacity (SC) was calculated via the following equation:

$$\text{SC}\,(\%) = \frac{\left(\text{OD}_{\text{blank}} - \text{OD}_{\text{sample}}\right)}{\text{OD}_{\text{blank}}} \times 100\%, \quad (2)$$

Measurements were repeated in triplicate.

2.3.2. Nitric Oxide (NO) Assay. Nitric oxide (NO) assay was assessed by Griess test to determine the NO concentration, which acts as an anti-inflammatory substance in the physiological environment. The gaseous NO was measured to employ a 2-step diazotization reaction. Briefly, dinitrogen trioxide (N_2O_3) was secreted from the acid-catalyzed formation of nitrous acid from nitrite reacts with sulfanilamide to produce diazonium ions. When they are combined with *N*-(1-naphthyl) ethylenediamine, they yield a chromophoric azo product that shows strong absorbance at 540 nm [16, 17]. In this study, RAW 264.7 cells (ATTC, USA) were seeded in 24-well plates at a density of 5×10^5 cells per well in 400 μL of DMEM media (Sigma Aldrich, St. Louis, MO) containing 5% fetal bovine serum (Sigma Aldrich, St. Louis, MO) and 1% antibiotics (penicillin/streptomycin/neomycin; Invitrogen, Carlsbad, CA), and the cells were incubated for 24 h at a humidified atmosphere of 5% CO_2 at 37°C. Then, 50 μL of samples (siRNP, CUR@siRNP, CUR@si-nRNP, and CUR in DMSO 10%) was added at the concentration of 100 μL/mL. Next, 50 μL of lipopolysaccharide (LPS; Sigma Aldrich, St. Louis, MO) was added. After 12 h, 50 μL of

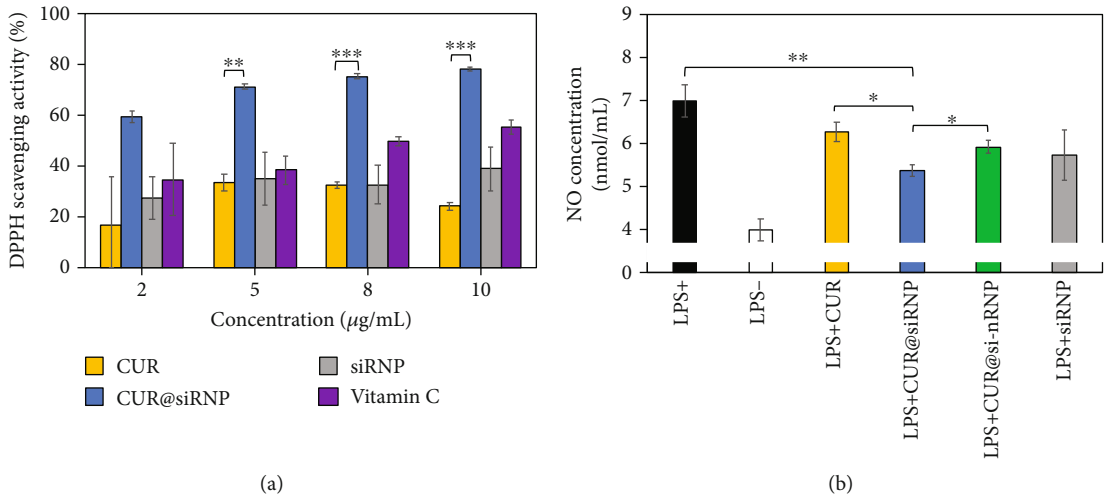

Figure 5: Bioactivities of CUR@siRNP. (a) The antioxidant activity of CUR, CUR@siRNP, and siRNP using DPPH assay. Vitamin C served as the positive control, while distilled water (DW) acted as the negative control. (b) The anti-inflammatory effect of CUR (curcumin in DMSO 10%), CUR@siRNP, CUR@si-nRNP, and siRNP via NO assay in the LPS-induced RAW 264.7 macrophage activation. Data are expressed as mean ± SD, $n = 3$, $^{*}p < 0.05$, $^{**}p < 0.01$, and $^{***}p < 0.001$.

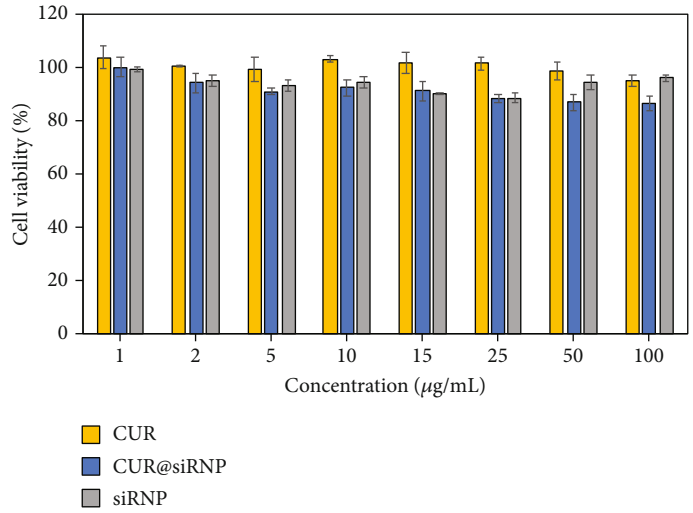

Figure 6: Cell viability of BAEC was determined by MTT assay. The concentration in the horizontal axis indicates the concentration of CUR, while the concentration of siRNP was 10 times higher than the concentration of CUR. Data are expressed as mean ± SD and $n = 3$.

Table 4: Table of pharmacokinetic parameters.

Pharmacokinetic parameter	Formulation	
	CUR	CUR@siRNP
Dose (mg/kg)	25	25
AUC (μg.h/mL)*	1.34 ± 0.09	2.79 ± 0.11
C_{max} (μg/mL)	0.69 ± 0.14	1.74 ± 0.08
T_{max} (h)	0.5	0.5
K_e (1/h)	0.71 ± 0.53	0.62 ± 0.14
$t_{1/2}$ (h)	1.34 ± 0.76	1.55 ± 0.25
V_d (mL/g)	37.01 ± 22.48	14.86 ± 2.61
Cl (mL/h)**	18.77 ± 0.98	8.98 ± 0.34

supernatant was collected and well-mixed with 50 μL Griess reagent containing 2% sulfanilamide, 0.2% N-(1-naphthylethylenediamine) dihydrochloride, and 5% acid phosphoric. The absorbance of each well was determined spectrophotometrically at a bandwidth of 540 nm. NO concentration was calculated using NO calibration curve constructed with $NaNO_2$ dilution. The wells without LPS acted as the negative control, while wells with no addition of samples were served as the positive control.

2.4. Cytotoxicity Evaluation. The cytotoxicity, based on cell metabolic activity alteration, was evaluated using 3-(4,5-dimethylthiazol-2-yl)-2,5-diphenyltetrazolium bromide (MTT; St. Louis, MO) assay. The yellow pigment of MTT was being reduced by living cells to purple formazan. Formazan particles are mostly insoluble in water; hence, a

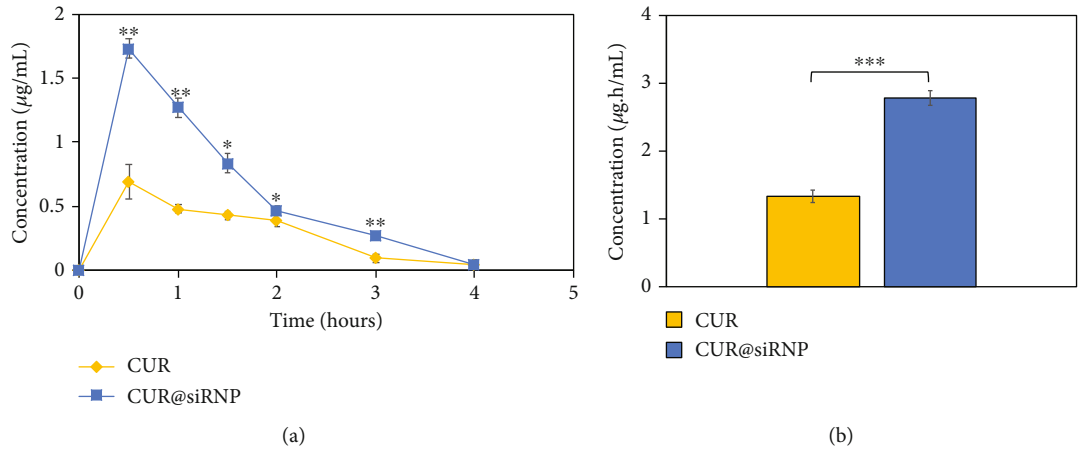

Figure 7: (a) Amount of curcumin in the plasma after oral administration of CUR (free curcumin) or CUR@siRNP. (b) AUC of curcumin in the plasma after oral administration of CUR (free curcumin) or CUR@siRNP. Data are expressed as mean ± SD, $n = 3$, $^{*}p < 0.05$, $^{**}p < 0.01$, and $^{***}p < 0.001$.

solubilization buffer was added to dissolve formazan particles. The absorbance of the solution was measured at 540 nm for the quantification of formazan, which is proportional to living cells. In this research, an MTT assay was performed on bovine aortic endothelial cells (BAEC from JCRB Cell Bank, Japan). BAEC was seeded in a 96-well plate, containing approximately 5×10^3 cells. After 24 h incubation, 10 μL of CUR, siRNP, and CUR@siRNP with various concentrations was added. The wells were incubated for another 24 h, and 5 μL of MTT solution was added to each well afterward. After 4 h incubation, 50 μL solubilization buffer was added to each well and left incubating overnight. The absorbance of each well was measured at 540 nm.

2.5. Pharmacokinetics of CUR@siRNP In Vivo. The 30 g adult male Swiss mice (Institute of Drug Quality Control Ho Chi Minh City) were acclimated at least 3 days before the experiments, and the mice were provided with free access to food and water. The animal experimental protocol was approved by the School of Biomedical Engineering, International University Ho Chi Minh. The mice were divided randomly into two groups (3 mice per group): CUR-treated group (CUR in carboxymethyl cellulose 0.5%) and CUR@siRNP-treated group. All groups were administered by oral gavage at a single dose of 25 mg/kg (Figure 2). The mice were anesthetized for collecting blood in heparin sodium-coated tube, and the plasma was obtained by centrifugation. Then, 50 μL of plasma and 100 μL mixture of acetonitrile and methanol (1 : 1) were added and vortexed for a minute. The mixtures were centrifuged at 11,200 g at 4°C for 10 min. CUR concentration in the supernatant was determined by fluorescence intensity with excitation and emission wavelengths of 425 nm and 597 nm, respectively. The plasma was frozen and stored at −80°C until further use. Pharmacokinetic parameters were estimated using the model-independent method. The terminal elimination rate constant (K_e) was estimated by a linear regression analysis of the terminal portion of the log-linear blood concentration-time profile of CUR. The terminal elimination half-life ($t_{1/2}$) was calculated from K_e using the formula $T_{1/2} = 0.693/K_e$. The maximum observed plasma concentration (C_{max}) and the time taken to reach it (T_{max}) were obtained from the curve plotting CUR concentration with time. The area under each drug concentration time curve (AUC, (ug.h)/mL) to the last data point was calculated by the linear trapezoidal rule and extrapolated to time infinity by the addition of C_{last}/K_e, where C_{last} is the concentration of the last measured plasma sample. The apparent body clearance (Cl) was calculated using the equation Cl = Dose/AUC. The apparent volume of distribution (V_d) was calculated by the equation V_d = Dose/(K_e.AUC).

2.6. Therapeutic Effect of CUR@siRNP in Colitis Mouse Model Induced by DSS. Colitis in mice was induced by 3% (wt/vol) dextran sodium sulfate (DSS, 5,000 Daltons; Fujifilm Wako Pure Chemicals, Osaka, Japan) supplemented in the drinking water for 7 d. The mice were randomized divided into 4 groups: healthy group, DSS-injured group, CUR-treated group, and CUR@siRNP-treated group. The equivalent doses of drugs (25 mg/kg) were orally administered daily during the 7 days of DSS treatment (Figure 3). The body weight changes were measured daily, while visible stool consistency and feces bleeding were assessed in the sacrifice day. Disease activity index (DAI) is the summation of stool consistency index (0–3), feces bleeding index (0–3), and weight loss index (0–4) (Table 1). After 7 days of treatment, the mice were sacrificed after anesthesia with xylazine (6 mg/kg) and zoletil (5 mg/kg). Then, the entire colon (from the cecum to the rectum) was collected. Colon length was measured and gently washed with physiological saline. After that, 1 cm of the middle section was used for histologic assessment. The histological score of the colon was evaluated using a microscope. Moreover, the histological score is the summation of crypt architecture (0–3), cellular infiltration (0–3), and goblet cell depletion (absent–0, present–1) (Table 2).

2.7. Statistical Analysis. All experiments were conducted at least thrice, and the data represent the mean ± SEM.

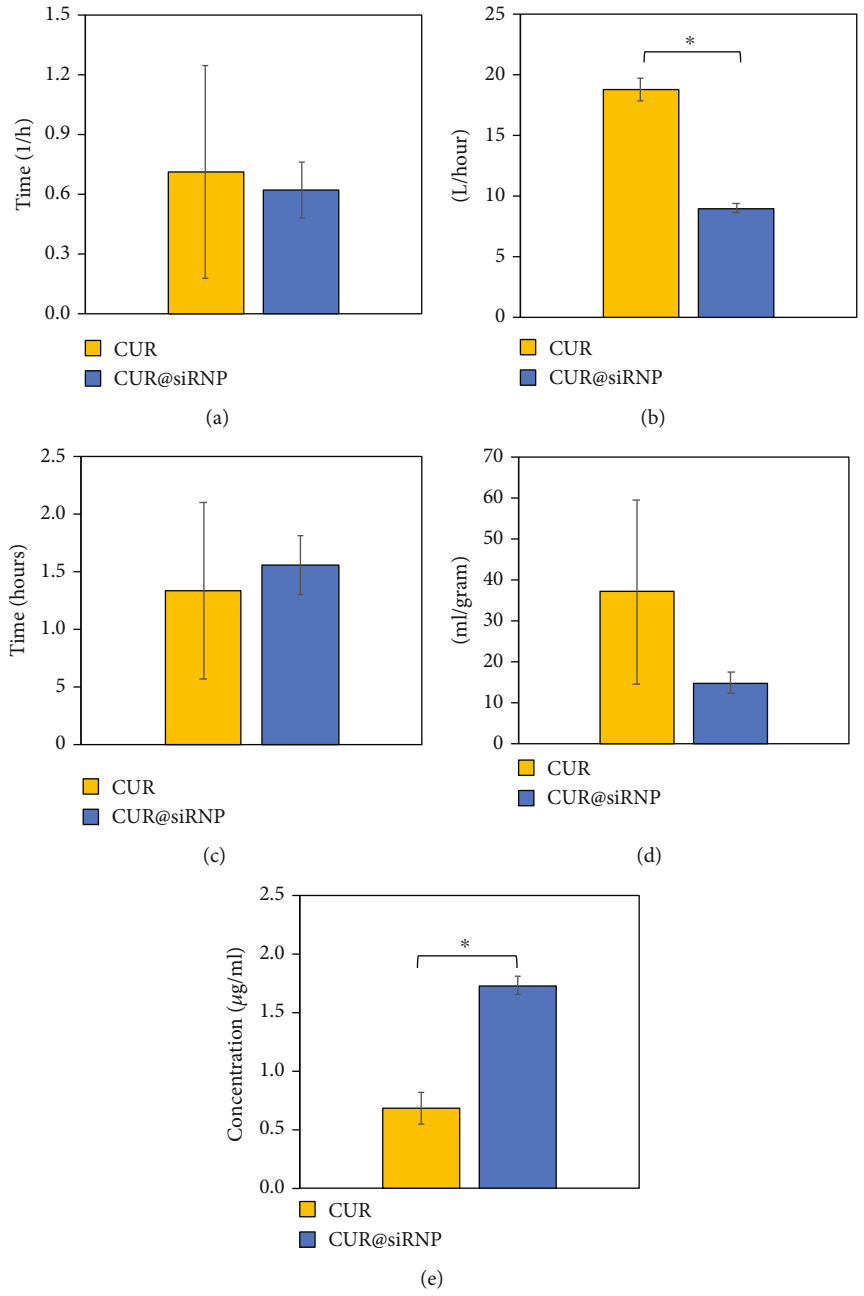

Figure 8: The comparison of pharmacokinetic parameters between CUR (free curcumin) and CUR@siRNP. (a) Elimination rate. (b) Clearance. (c) Half-life. (d) Volume distribution. (e) Maximum concentration. Data are expressed as mean ± SD, $n = 3$, and $^{*}p < 0.01$.

Statistical comparisons were performed using one-way analysis of variance (ANOVA) followed by Student's t-test using Microsoft Excel. The results were analyzed and considered statistically significant differences when $p < 0.05$ using a two-tailed t-test.

3. Results and Discussion

3.1. Characteristics of CUR@siRNP. CUR is an antioxidant substance with extremely poor solubility in an aqueous solution (<8 μg/mL) [22]; hence, the CUR sample remained insoluble in water, evidenced by small particle accumulated at the bottom of the centrifuge tube (Figure 4(a), left). Meanwhile, the CUR@siRNP solution had dark-brown colour without any precipitation (Figure 4(a), right), indicating the improvement of CUR solubility in water. As the colour became darker, it may be due to the change in particle size. Next, the size of CUR@siRNP was evaluated by DLS measurement. As shown in Figure 4(b) and Table 3, siRNP size slightly increased from 122 ± 1 nm to 142 ± 1 nm in the CUR@siRNP sample, implying that CUR was successfully encapsulated within the siRNP. In this study, CUR@siRNP size was under 200 nm, which is preferable to a complex drug delivery device to be efficient to achieve the enhanced

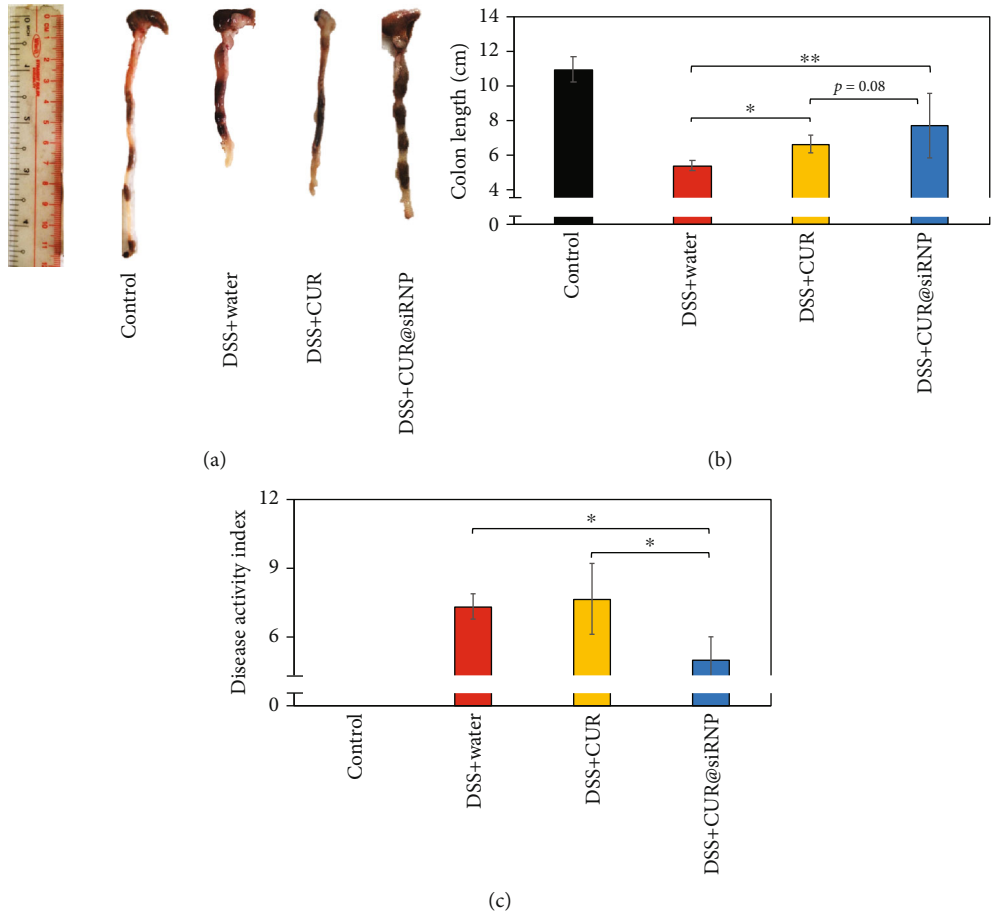

FIGURE 9: The therapeutic effect of CUR@siRNP in colitis mice. (a) The colon of mice after 7 days of treatment. (b) Changes in colon length. (c) Changes in DAI. DAI is the summation of stool consistency index (0–3), feces bleeding index (0–3), and weight loss index (0–4). Data are expressed as mean ± SD, $n = 5$, $^{*}p < 0.05$, and $^{**}p < 0.01$.

permeability and retention effect for the passive targeting in the inflammatory tissue [23]. In addition, monodispersity was observed with a low PDI (polydispersity index) value (<0.3), suggesting a narrow size distribution of siRNP and CUR@siRNP. Next, the encapsulation efficiency (EE) and drug loading capacity (LC) of CUR@siRNP were measured using UV-VIS spectrophotometer. In this study, the EE and LC of CUR@siRNP were 70% and 7%, respectively (Table 3). The use of siRNP helps increase CUR solubility, enabling it to overcome biological barriers that are especially easier to absorb by intestinal epithelial cells.

3.2. Bioactivities of CUR@siRNP. CUR is a natural antioxidant agent; however, due to low bioavailability, it exerted a low antioxidant effect by scavenging DPPH radical (Figure 5(a)). Meanwhile, siRNP contains both ROS scavenging moiety of nitroxide radical (TEMPO) and a drug absorptive moiety of silica for protection against oxidative damage while enhancing stability of CUR through oral delivery. It has been reported that nitroxide radical TEMPO strongly scavenges superoxide and hydroxyl radicals [24, 25], which are higher generated in the inflammatory tissues. Therefore, siRNP acts as not only a nanocarrier but also as a ROS scavenging agent to increase the antioxidant activity of CUR. At 10 μg/mL concentration, the CUR@siRNP sample had the highest DPPH scavenging activity (78.2%) compared to both CUR (24.4%) and siRNP (39.1%), suggesting that the synergistic effect was observed. This result indicated siRNP is an ideal nanocarrier for CUR, by enhancing CUR's natural antioxidant profile. Next, we investigated the anti-inflammatory activity *in vitro* using the RAW 264.7 cell model. NO is considered as a biomarker for proinflammatory due to the activation by macrophages. In this assay, NO was stimulated by RAW 264.7 cells due to the introduction of LPS *in vitro* (Figure 5(b)). The level of NO is inversely proportional to the anti-inflammatory activities of the added samples. Both CUR and siRNP showed the effect to suppress the NO level in LPS-activated macrophage cells. Interestingly, CUR@siRNP demonstrated a significant inhibition in NO level as compared to CUR and siRNP alone. These results indicated that CUR@siRNP presents higher antioxidant and anti-inflammatory activity *in vitro* as compared to free CUR.

3.3. Drug Cytotoxicity. After evaluating the antioxidant and anti-inflammatory activities of CUR@siRNP *in vivo*, the cytotoxicity was investigated using MTT assay against BAEC cell line. As shown in Figure 6, at low concentration, CUR@siRNP showed no significant difference in cell viability than

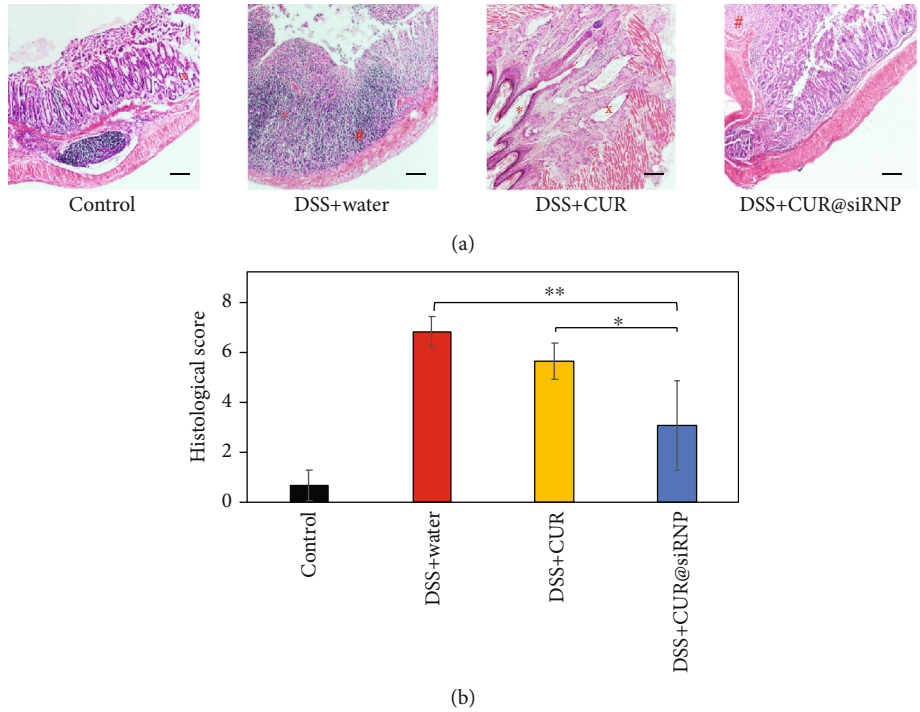

Figure 10: The histological assessment of colon after treatment. (a) Histology of 7 μm thick colonic sections by hematoxylin and eosin staining. Scale bar = 100 μm. *: distortion of crypt architecture. $^{\#}$: cellular infiltration. ^{x}: goblet cell depletion. (b) Histological score of colon section after 7 days of DSS treatment. Data are expressed as mean ± SD, $n = 5$, $^{*}p < 0.05$, and $^{**}p < 0.01$.

CUR and siRNP-treated cells. At higher concentrations, both CUR@siRNP and siRNP demonstrated a slight toxicity than free CUR. However, all CUR@siRNP and siRNP obtained 86% or more in cell viability even at high concentration (100 μg/mL), which suggested a low toxicity of CUR@siRNP against BAEC cell. It should be noticed that the concentration of siRNP was 10 times higher than the concentration of CUR. Several nanomaterials have been reported with high toxicity via inducing the generation of ROS [26]. Our previous study suggested that ROS scavenging nanoparticle could suppress the toxicity of the nanomaterial itself [27]. Therefore, CUR@siRNP was shown with low cytotoxicity, while promoting beneficial biological effects of CUR, which is highly desirable and promising as an anti-inflammatory therapeutic approach.

3.4. Pharmacokinetics of CUR@siRNP In Vivo. Since CUR@siRNP significantly improved the solubility of CUR, we continue to evaluate the bioavailability of orally administered CUR@siRNP *in vivo* mouse model (Figure 2). In this study, the pharmacokinetics was evaluated, and the basic parameters were typically shown in Table 4. The pharmacokinetic properties of CUR and CUR@siRNP were presented as follows.

Values reported as mean ± S.D. ($n = 3$). AUC: area under the plasma concentration–time curve; C_{max}: peak concentration; T_{max}: time to reach peak concentration; K_e: constant of elimination; $t_{1/2}$: mean half-life; V_d: apparent volume of distribution; Cl: clearance. Significant difference of CUR@siRNP versus CUR ($^{*}p < 0.05$ and $^{**}p < 0.01$).

Area Under Curve (AUC): the AUC of CUR was quite low (1.34 ± 0.09 μg.h/mL), indicating an extremely low drug absorption and internalization in the bloodstream via the intestine after oral administration. Meanwhile, the AUC value of CUR@siRNP was significantly higher (2.79 ± 0.11 μg.h/mL), which demonstrated the concentration of drugs in the bloodstream over time had been greatly improved compared to CUR aqueous suspension ($p < 0.001$) (Figures 7(a) and 7(b)).

To compare the retention of CUR and CUR@siRNP, the pharmacokinetic parameters were also described in Table 4 and Figure 8.

C_{max} and T_{max}: after the oral administration, both drugs were adsorbed quickly and achieved the highest plasma drug concentration after 0.5 h. While the maximum concentration of CUR was only 0.69 ± 0.14 μg/mL, which was quite low, the concentration of CUR@siRNP was increased 2.8-fold (1.74 ± 0.078 μg/mL) at max, indicating siRNP has improved the absorption of CUR into the bloodstream.

Elimination rate (K_e) and half-life ($t_{1/2}$): coefficients indicate the rate of elimination of the drug and the time it takes for the drug concentration to be half of its highest concentration. The elimination rate of CUR@siRNP was improved, showing that the CUR in nanoparticles eliminated slower than the CUR sample. At the same time, the $t_{1/2}$ of CUR@siRNP was increased up to 1.5 h. It suggested that the siRNP could improve the elimination time of CUR in mice, enhancing the effects of CUR in treatment.

Clearance: this feature indicates the elimination of the drug from the body. The clearance level was 18.77 ± 0.98

(mL/h) for the CUR-treated mice, which suggested that the drug digests out very quickly. CUR@siRNP clearance level was 8.98 ± 0.34 (mL/h), which was smaller and decreased 1.7-fold compared to CUR. It demonstrated that the drug was excreted slowly, staying in the body in a long period, and may exert the drug effect for a longer time. These data indicated that CUR@siRNP not only could improve the level of CUR in the bloodstream after oral administration but also prolonged the retention of CUR, which is anticipated the higher therapeutic treatment *in vivo* model.

3.5. Therapeutic Effect of CUR@siRNP in Colitis Mouse Model Induced by DSS. It was confirmed that the antioxidant and anti-inflammatory activities and pharmacokinetics profile of CUR@siRNP were remarkably improved compared to free CUR. Next, we evaluated the therapeutic anti-inflammatory effect *in vivo* using the DSS-induced colitis mouse model. DSS-induced colitis is a well-known model of inflammation in the colon, characterized by high disease activity index (DAI) and shortening colon length after 7 d treatment of DSS [24]. The shortening of colon length is an indicator of inflammation in DDS-induced colitis mice. As the result, the colon length of DSS-treated mice was significantly shortened (5.3 ± 0.3 cm), while the healthy control group was 10.9 ± 0.8 cm, indicating that the DSS-treated mice formed severe colitis (Figures 9(a) and 9(b)). Both mice treated with CUR and CUR@siRNP showed a significant improvement in colon length as compared to DSS-induced colitis mice ($^{*}p < 0.05$ and $^{**}p < 0.01$, respectively). Although the colon length of the CUR@siRNP-treated group (7.7 ± 1.2 cm) was longer than the CUR-treated group (6.6 ± 0.5 cm), a significant difference was not observed ($p = 0.08$). This result suggested that the CUR@siRNP was effectively suppressed the inflammation and preserved the colon length. In addition, the disease activity index (DAI), which is the sum of body weight loss, stool consistency, and bleeding, was evaluated. The DAI of the CUR@siRNP-treated group was the lowest compare to other treated groups, showing that siRNP improved its therapeutic effect of CUR (Figure 9(c)). More specifically, the CUR@siRNP-treated group reduced the bleeding in the colon and diarrhea levels of colitis mice. Therefore, it demonstrated that oral administration of CUR@siRNP could suppress the inflammatory damage in colitis mice.

Finally, the histology was examined to evaluate the therapeutic effect of CUR@siRNP in DSS-induced colitis mice. When the histology of colitis tissue was examined, moderate crypt distortion and cellular infiltration were shown in mice treated with DSS (Figure 10(a)). While treatment with CUR did not show any effect at all, the CUR@siRNP-treated mice showed less crypt architecture damage and cellular infiltration. Therefore, the histological score of the CUR@siRNP-treated group showed a significant difference compared to other groups (Figure 10(b)), indicating the improvement of therapeutic effect of CUR@siRNP on treating the inflammation in colitis mice. These results suggested that siRNP could enhance the anti-inflammatory efficacy of CUR not only by improving the bioavailability and distribution of CUR but also by its ROS scavenging activity.

4. Conclusions

In this study, siRNP was utilized to deliver CUR for a better inflammatory therapeutic effect. Possessing ROS scavenging feature, siRNP significantly improved not only the solubility and but also the antioxidant and anti-inflammatory activities of CUR. Additionally, oral administration of CUR@siRNP increased the concentration of CUR in blood and suppressed the CUR clearance significantly, resulting in a better pharmacokinetic profile of CUR *in vivo*. Consequently, CUR@siRNP effectively improved disease activity index and colonic injury in the DSS-induced colitis model mice, indicating that siRNP demonstrates a great potential in bioavailability improvement of various hydrophobic drugs. Further investigation and development are needed to show a firm demonstration of CUR@siRNP potential in treating chronic inflammation.

Data Availability

The data used to support the findings of this study are available from the corresponding author upon request.

Conflicts of Interest

The authors have no competing financial interests to declare.

Acknowledgments

This work was supported by the Vietnam National University Ho Chi Minh City (VNU-HCM) under grant number C2019-18-24. The authors also would like to thank Prof. Yukio Nagasaki and Ms. Hao Thi Tran for kindly giving the polymer.

References

[1] L. Ferrucci and E. Fabbri, "Inflammageing: chronic inflammation in ageing, cardiovascular disease, and frailty," *Nature Reviews. Cardiology*, vol. 15, no. 9, pp. 505–522, 2018.

[2] D. Furman, J. Campisi, E. Verdin et al., "Chronic inflammation in the etiology of disease across the life span," *Nature Medicine*, vol. 25, no. 12, pp. 1822–1832, 2019.

[3] S. J. Forrester, D. S. Kikuchi, M. S. Hernandes, Q. Xu, and K. K. Griendling, "Reactive oxygen species in metabolic and inflammatory signaling," *Circulation Research*, vol. 122, no. 6, pp. 877–902, 2018.

[4] M. Mittal, M. R. Siddiqui, K. Tran, S. P. Reddy, and A. B. Malik, "Reactive oxygen species in inflammation and tissue injury," *Antioxidants & Redox Signaling*, vol. 20, no. 7, pp. 1126–1167, 2014.

[5] J. Trujillo, Y. I. Chirino, E. Molina-Jijón, A. C. Andérica-Romero, E. Tapia, and J. Pedraza-Chaverrí, "Renoprotective effect of the antioxidant curcumin: recent findings," *Redox Biology*, vol. 1, no. 1, pp. 448–456, 2013.

[6] Y. He, Y. Yue, X. Zheng, K. Zhang, S. Chen, and Z. Du, "Curcumin, inflammation, and chronic diseases: how are they linked?," *Molecules*, vol. 20, no. 5, pp. 9183–9213, 2015.

[7] S. Thangavel, T. Yoshitomi, M. K. Sakharkar, and Y. Nagasaki, "Redox nanoparticles inhibit curcumin oxidative degradation and enhance its therapeutic effect on prostate cancer," *Journal of Controlled Release*, vol. 209, pp. 110–119, 2015.

[8] C. Moorthi and K. Kathiresan, "Curcumin–piperine/curcumin–quercetin/curcumin–silibinin dual drug-loaded nanoparticulate combination therapy: a novel approach to target and treat multidrug-resistant cancers," *Journal of Medical Hypotheses and Ideas*, vol. 7, no. 1, pp. 15–20, 2013.

[9] S. Gelperina, K. Kisich, M. D. Iseman, and L. Heifets, "The potential advantages of nanoparticle drug delivery systems in chemotherapy of tuberculosis," *American Journal of Respiratory and Critical Care Medicine*, vol. 172, no. 12, pp. 1487–1490, 2005.

[10] E. M. Pridgen, F. Alexis, and O. C. Farokhzad, "Polymeric nanoparticle drug delivery technologies for oral delivery applications," *Expert Opinion on Drug Delivery*, vol. 12, no. 9, pp. 1459–1473, 2015.

[11] M. Kanai, A. Imaizumi, Y. Otsuka et al., "Dose-escalation and pharmacokinetic study of nanoparticle curcumin, a potential anticancer agent with improved bioavailability, in healthy human volunteers," *Cancer Chemotherapy and Pharmacology*, vol. 69, no. 1, pp. 65–70, 2012.

[12] K. Tai, M. Rappolt, L. Mao, Y. Gao, X. Li, and F. Yuan, "The stabilization and release performances of curcumin-loaded liposomes coated by high and low molecular weight chitosan," *Food Hydrocolloids*, vol. 99, p. 105355, 2020.

[13] C. Mohanty, M. Das, and S. K. Sahoo, "Emerging role of nanocarriers to increase the solubility and bioavailability of curcumin," *Expert Opinion on Drug Delivery*, vol. 9, no. 11, pp. 1347–1364, 2012.

[14] L. B. Vong, S. Kimura, and Y. Nagasaki, "Newly designed silica-containing redox nanoparticles for oral delivery of novel TOP2 catalytic inhibitor for treating colon cancer," *Advanced Healthcare Materials*, vol. 6, no. 20, article 1700428, 2017.

[15] T.-H. T. Nguyen, N.-T. Trinh, H. N. Tran et al., "Improving silymarin oral bioavailability using silica-installed redox nanoparticle to suppress inflammatory bowel disease," *Journal of Controlled Release*, 2020.

[16] J. N. Sharma, A. Al-Omran, and S. S. Parvathy, "Role of nitric oxide in inflammatory diseases," *Inflammopharmacology*, vol. 15, no. 6, pp. 252–259, 2007.

[17] M. B. Grisham, G. G. Johnson, and J. R. Lancaster Jr., "Quantitation of nitrate and nitrite in extracellular fluids," *Methods in Enzymology*, vol. 268, pp. 237–246, 1996.

[18] L. B. Vong, T. Tomita, T. Yoshitomi, H. Matsui, and Y. Nagasaki, "An orally administered redox nanoparticle that accumulates in the colonic mucosa and reduces colitis in mice," *Gastroenterology*, vol. 143, no. 4, pp. 1027–1036.e3, 2012.

[19] L. B. Vong, T. Yoshitomi, K. Morikawa, S. Saito, H. Matsui, and Y. Nagasaki, "Oral nanotherapeutics: effect of redox nanoparticle on microflora in mice with dextran sodium sulfate-induced colitis," *Journal of Gastroenterology*, vol. 49, no. 5, pp. 806–813, 2014.

[20] J. J. Kim, M. S. Shajib, M. M. Manocha, and W. I. Khan, "Investigating intestinal inflammation in DSS-induced model of IBD," *JoVE (Journal of Visualized Experiments)*, no. 60, article e3678, 2012.

[21] H. Laroui, S. A. Ingersoll, H. C. Liu et al., "Dextran sodium sulfate (DSS) induces colitis in mice by forming nano-lipocomplexes with medium-chain-length fatty acids in the colon," *PLoS One*, vol. 7, no. 3, article e32084, 2012.

[22] K. Suresh and A. Nangia, "Curcumin: pharmaceutical solids as a platform to improve solubility and bioavailability," *Cryst Eng Comm*, vol. 20, no. 24, pp. 3277–3296, 2018.

[23] R. Singh and J. W. Lillard Jr., "Nanoparticle-based targeted drug delivery," *Experimental and Molecular Pathology*, vol. 86, no. 3, pp. 215–223, 2009.

[24] M. Lewandowski and K. Gwozdzinski, "Nitroxides as antioxidants and anticancer drugs," *International Journal of Molecular Sciences*, vol. 18, no. 11, p. 2490, 2017.

[25] A. M. Samuni, W. DeGraff, M. C. Krishna, and J. B. Mitchell, "Nitroxides as antioxidants: tempol protects against EO9 cytotoxicity," *Molecular and Cellular Biochemistry*, vol. 234/235, no. 1, pp. 327–333, 2002.

[26] R. P. Singh and P. Ramarao, "Accumulated polymer degradation products as effector molecules in cytotoxicity of polymeric nanoparticles," *Toxicological Sciences*, vol. 136, no. 1, pp. 131–143, 2013.

[27] L. B. Vong, M. Kobayashi, and Y. Nagasaki, "Evaluation of the toxicity and antioxidant activity of redox nanoparticles in zebrafish (*Danio rerio*) embryos," *Molecular Pharmaceutics*, vol. 13, no. 9, pp. 3091–3097, 2016.